SAND80-8212
Unlimited Release

Design and Operation of Thermal Convention Loops for Corrosion Testing in Molten $NaNO_3$-KNO_3

W. S. Winters, R. W. Bradshaw, F. W. Hart

Prepared by Sandia Laboratories, Albuquerque, New Mexico 87185
and Livermore, California 94550 for the United States Department
of Energy under Contract DE-AC04-76DP00789.

Printed June 1980

Sandia Laboratories

SF 2900 Q(7-73)

Issued by Sandia Laboratories, operated for the United States Department of Energy by Sandia Corporation.

NOTICE

Printed in the United States of America
Available from
National Technical Information Service
U. S. Department of Commerce
5285 Port Royal Road
Springfield, VA 22161
Price: Printed Copy $4.50 ; Microfiche $3.00

SAND80-8212
Unlimited Release
Printed June 1980

DESIGN AND OPERATION OF THERMAL CONVECTION LOOPS FOR CORROSION TESTING IN MOLTEN $NaNO_3$ - KNO_3

W. S. Winters
R. W. Bradshaw
F. W. Hart
Sandia National Laboratories, Livermore, CA

ABSTRACT

Convective loop experiments are a valuable and relatively inexpensive method of assessing the effects of mass transport and a fully operational temperature gradient on molten salt materials compatibility. This report documents the design, construction, operation, and preliminary results of three molten draw salt corrosion loop experiments conducted at SLL. The loops were constructed from 304 SS, 316 SS, and Incoloy 800. This effort was undertaken to support the DOE program for Thermal Energy Storage for Solar Thermal Applications.

CONTENTS

	Page
I. Introduction and Background	9
A. Objective	9
B. The TESSTA Program	9
C. Molten Salts in Solar Thermal Power Systems	10
D. Compatibility of Structural Alloys with Molten Nitrates	11
II. Description of Convective Loop Experiments	11
A. General Design Features	11
B. Specific Design Features	12
1. 304 SS Loop	16
2. 316 SS Loop	16
3. Incoloy 800 Loop	16
C. Operating Procedures	21
D. Flowrate Estimates	21
III. Materials Testing	23
A. Experimental Design and Procedure	23
B. Preliminary Results	24
IV. Future Activities	26
V. Conclusions	29
VI. REFERENCES	31
APPENDIX A- MATERIALS LIST AND COST ESTIMATE FOR A TYPICAL CONVECTIVE LOOP	33

ILLUSTRATIONS

No.		Page
1	Bouyancy driven flow in a convective loop	13
2	Photograph of 304 SS loop	14
3	Photograph of 316 SS and Incoloy 800 loops	15
4	Schematic of 304 SS loop	18
5	Schematic of 316 SS loop	19
6	Schematic of Incoloy 800 loop	20
7	Microstructure of 304 SS after 1977 Hours at 600°C (1112°F)	25
8	Weight changes of 316 SS and IN800 at 640°C (1184°F)	27
9	Corrosion products on 316 SS after 1005 Hours at 640°C (1184°F)	28

TABLES

No.		Page
I	STEADY STATE LOOP TEMPERATURE DISTRIBUTIONS	17
II	LOOP VELOCITY ESTIMATES FROM FIRST LAW ANALYSIS	22
III	CHEMICAL ANALYSIS OF SALT SAMPLES FROM 304 SS LOOP	26

DESIGN AND OPERATION OF THERMAL CONVECTION LOOPS FOR MATERIALS TESTING IN MOLTEN SALTS

I. Introduction and Background

A. Objective

The purpose of this report is to:

1. Document the design, construction, and operation of three convective loops used to assess the influence of mass transport and a temperature gradient on the compatibility of structural alloys in molten draw salt.

2. Report preliminary corrosion results from the convective loop experiments.

B. The TESSTA Program

Sandia Laboratories (SL) has been designated by the Division of Energy Storage (STOR) within the Department of Energy (DOE) as Lead Laboratory in charge of implementing the program for Thermal Energy Storage for Solar Thermal Applications (TESSTA). SL Lead Laboratory responsibilities include identifiying the important technical issues associated with thermal energy storage for solar thermal applications. In addition, SL plans activities and determines resource requirements necessary to resolve these technical issues in a timely manner. Private industry, universities, and in some cases national laboratories perform the required activities as operating contractors with SL performing only that generic R & D necessary for initiation, support, and management of the program.

One of the key elements for FY80 in the TESSTA Program is the evaluation of molten salt as a possible heat transfer fluid and thermal energy storage medium in solar thermal power systems. Studies to characterize molten salt behavior and to assess compatibility with candidate containment materials have been initiated. As part of the effort in molten salt materials compatibility studies, SL conducted an in-house effort to design, build, and operate prototype convective loops for the purpose of collecting long term corrosion data. The corrosion data will be used to aid in selection of construction material for solar systems. A secondary objective of this study was to obtain knowledge and experience in loop development and testing to be transfered directly to contractors in future salt/ materials studies. Every effort was made to perfect the loop design so that future loops can be built quickly and economically with commonly available materials (pipe, insulation, heaters, controllers, etc.).

C. Molten Salts in Solar Thermal Power Systems

A number of solar thermal concepts including the central receiver (1, 2), line focus (3, 4), and other distributed collector concepts are currently being studied by DOE as a means of supplying large quantities of thermal energy at high temperatures for process heat or electric power generation needs. In these concepts solar energy striking the earth is intercepted by a system of heliostats (sun tracking mirrors) and reflected onto a receiver. The receiver is a heat exchanger, which absorbs the redirected solar energy and transfers it to a circulating working fluid. The thermal energy carried by the working fluid is then available as input to an electric power generation system (EPGS) such as a Steam-Rankine power plant, or as heat for an industrial process.

Depending on the specific application, it may be necessary to store a portion of the collected thermal energy for later use. Storage is accomplished by directing the hot receiver working fluid to an energy storage subsystem (see References 5-7 for examples of thermal energy storage techniques) where the thermal energy is absorbed and stored for later use by the EPGS or the industrial process. Storage in a solar thermal facility acts as a thermal capacitance which can effectively isolate the EPGS or process heat sink from potentially harmful transients induced by clouds passing over the collector field. Thermal energy retreived from storage can also permit plant operations to continue into periods of the day or night when solar insolation is insufficient to operate the plant directly from receiver heat.

Molten nitrate salt mixtures (predominately $NaNO_3$ and KNO_3 mixtures) have been identified as being potentially attractive for use in solar thermal systems (1, 2). These salts can be used as both a receiver working fluid and energy storage medium, thereby eliminating the need for a costly heat exchanger interface between the receiver and storage subsystems. Draw salt is particularly attractive in solar thermal applications requiring large amounts of thermal energy storage, due to its low cost and the reduction in storage media and tankage costs resulting from its relatively high energy density. The relatively low vapor pressure of draw salt permits systems to operate near atmospheric pressures thereby avoiding the expense of high pressure containment.

Initial program emphasis in utilizing molten salt for solar thermal power applications has been in the development of the central receiver concept proposed by Martin Marietta (2). In this concept, molten nitrate salt circulates through the system (pipes, heat exchangers, pumps, valves, tanks, etc.) over a temperature range from 288°C (550°F) to 566°C (1050°F). The upper end of the temperature range is sufficient to allow a state-of-the-art Steam/Rankine EPGS to operate directly from the solar facility.

For the molten salt central receiver concept to be viable, a complete family of containment materials must be identified which combine minimum cost, adequate strength and corrosion resistance in each temperature regime in the system. These materials must be sufficiently corrosion resistant to permit reliable operation of the solar facility over its design life of 30 years.

D. Compatibility of Structural Alloys with Molten Nitrates

Although interest in solar thermal applications of molten nitrate salts is quite recent, this family of salts has been used as heat transfer fluids in the chemical processing industry. The salt mixture most widely used in these applications has been a salt mixture containing $NaNO_2$ (40% $NaNO_2$, 53% KNO_3, and 7% $NaNO_3$ by weight), rather than exclusively nitrate salts. Operating temperatures were somewhat lower than solar system requirements. Corrosion data resulting from these applications have not been systematically reported in the literature but some results have been summarized by Bohlmann (13). It appears that both stainless steels and nickel-base alloys corrode less than 25 μm/ year (1 mil/year) at 540°C (1004°F).

Recent corrosion studies undertaken to support solar thermal applications indicate relatively slow oxidation of highly alloyed structural materials in molten nitrate-nitrite mixtures and in molten nitrates at maximum temperatures of 550°C (1022°F). Type 316 stainless steel displays weight gains of about 2-3 mg/cm^2 after several thousand hours (2, 14). Type 310 SS behaves similarily (14) as does Incoloy 800 (2). The corrosion products on these iron-base alloys were generally the same, consisting of a duplex oxide layer a few microns thick which contained a layer of magnetite, Fe_3O_4, over an iron-chromium spinel layer. Inconel 600, a nickel-base alloy containing 15% Cr, displayed somewhat more surface scaling, as well as internal oxidation (15).

Although the results of isothermal immersion tests indicate that corrosion rates of high chromium alloys, such as the 300-series stainless steels and Incoloy 800, are quite slow, these tests revealed an accumulation of chromium in the melt (14, 15). Given that alloying elements or their corrosion products are soluble in the melt, thermal gradient mass transfer effects must be considered. Mass transfer effects could accelerate corrosion as well as cause deposits to form in the colder parts of heat exchanger circuits.

Results recently reported for 316 SS in a thermal convection loop containing 40% $NaNO_2$, 53% KNO_3 and 7% $NaNO_3$ described a serious corrosion problem. Rapid dissolution of the alloy in the high temperature section and deposition of metallic elements in the cold section was observed (17). Over a period of 5000 hours, at a maximum temperature of 550°C (1022°F), 316 SS samples lost 40 mg/cm^2. The corrosion rate was linear with time, indicating a lack of protective behavior by surface layers, and was extrapolated as 75 μm/yr (3 mil/yr). The rate of accumulation of chromium in the melt was also linear with time.

II. Description of Convective Loop Experiments

A. General Design Features

The logical and convenient first step in assessing molten salt materials compatibility consists of immersing metal samples in isothermal salt baths at various temperatures over extended periods of time. Samples withdrawn at predetermined intervals are weighed and examined metallographically. These static isothermal "hot soak" tests are useful as a screening process in identifying materials for further evaluation.

The utilization of convective loops represents a logical second step in assessing molten salt materials compatibility. Convective loops enable one to determine the influence of salt mass transport and temperature gradients on the corrosion characteristics of a particular containment material. As a result, convective loop tests more closely simulate an actual operating system, although the effects of thermal cycling and high flowrates are not included.

The most extensive use of thermal convection loops for materials testing has been concerned with breeder reactor development where liquid metals or molten salts have been proposed as heat transfer fluids. The corrosion behavior of alloys has been studied in liquid sodium (16, 18), molten alkali metal fluorides (19, 20) and molten halide mixtures (21) in this type of apparatus. Thermal convection loops have also been used to study mass transport-related corrosion in molten carbonate salts (22) and molten sodium hydroxide (23).

The principle behind convective loop testing is illustrated in Figure 1. Heat is applied to one leg (hot leg) of the convective loop, increasing the temperature and reducing the density of the salt in the hot leg. The density decrease results in a bouyancy induced flow pattern in the direction shown. In order for the loop to operate at steady state, an equal amount of heat must be dissipated from the cold leg. This cooling results in an increase in salt density which causes the salt to flow downward through the cold leg completing a cyclic flow pattern in the loop. Bouyancy induced loop flows are described analytically in References 8-12.

To conduct corrosion research, samples may be suspended at various points along the vertical hot and cold legs and retrieved at pre-determined intervals. In addition, the loops may be drained at the conclusion of testing and sectioned for metallographic analysis to provide additional corrosion data. In so doing, it is possible to evaluate the corrosion behavior over a complete temperature range. By controlling the heat input to the loop and judiciously applying insulation it is possible to adjust the temperature distribution. Once steady state flow conditions are achieved the loop may be left unattended for extended periods of time. Since no pumps or valves are required, the experiment is simple and economical to construct. Furthermore, no foreign pump or valve materials are introduced into the flow. In the present molten draw salt corrosion experiments, the loops, thermocouple sheaths, and sample fixtures were constructed from the same material as the samples. This insured that the observed corrosion mechanisms were characteristic of the particular draw salt/metal sample combination.

B. Specific Design Features

In the present program three loops were constructed and tested: 1) a 304 stainless steel/molten nitrate salt loop, 2) a 316 stainless steel/molten nitrate salt loop, and 3) an Incoloy 800/molten nitrate salt loop. Incoloy 800 and 316 stainless steel are currently the leading candidates for high temperature 566°C (1050°F) molten nitrate salt containment. The loops were left open to the atmosphere. All three loops were electrically heated and passively cooled via free convection to the surroundings. Photographs of the loop experiments appear in Figures 2 and 3.

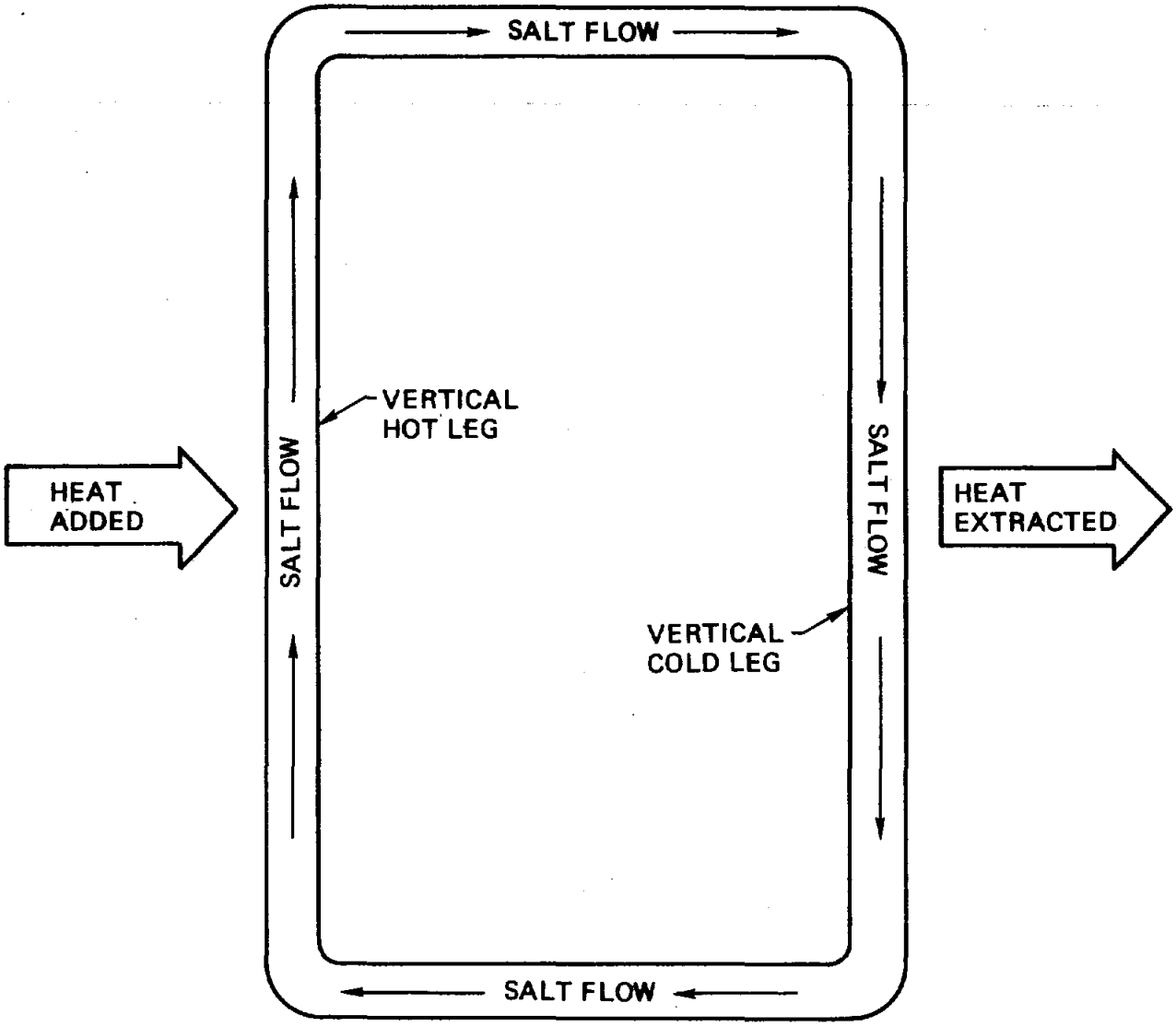

Figure 1. Bouyancy Driven Flow in a Convective Loop

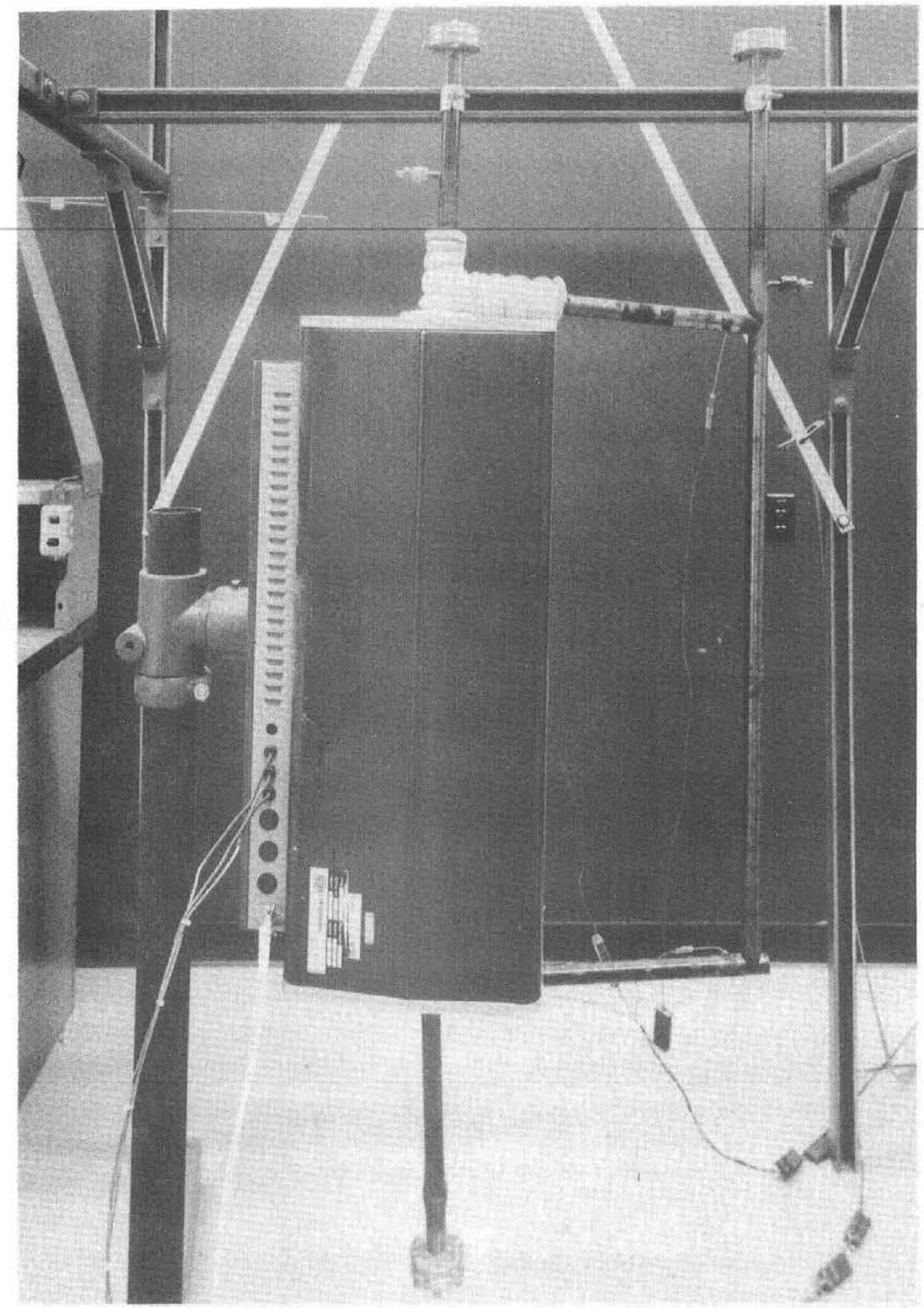

Figure 2. Photograph of 304 SS Loop

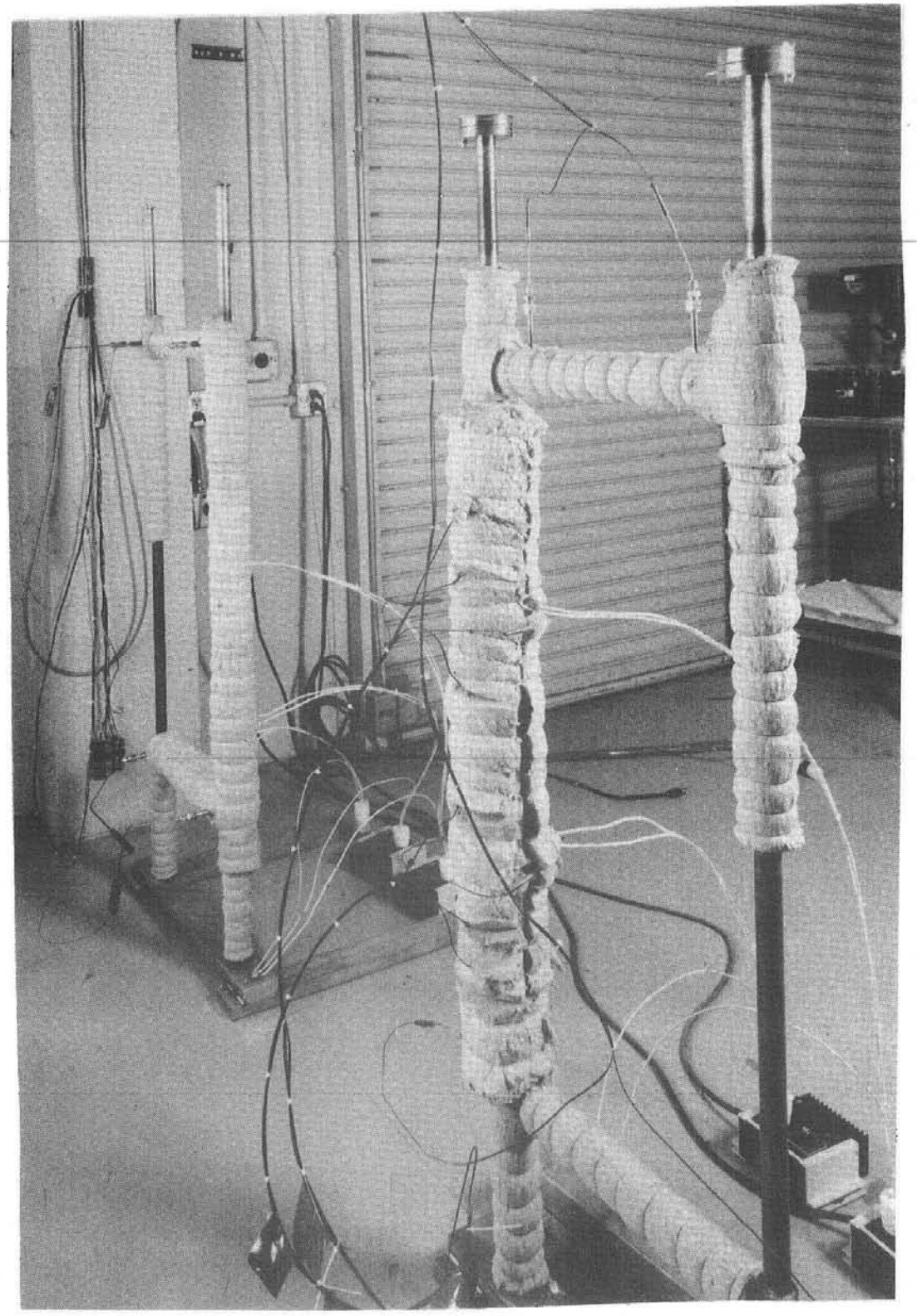

Figure 3. Photograph of 316 SS (Foreground) and Incoloy 800 Loops

1. 304 SS Loop

A schematic of the 304 SS loop is shown in Figure 4. In addition to providing useful corrosion data, this loop served as a prototype for the design, construction, and operation of subsequent loops. A 3-zone temperature controlled tube furnace was used to provide flexibility in the adjustment of the loop temperature distribution. On the later 316 SS and Incoloy 800 loops, this relatively costly piece of equipment was replaced by lower cost, "clam shell" heaters covered with insulation. Steady state temperature was monitored from four (T_{f1}, T_{f2}, T_{f3}, T_{f4}) permanently installed thermocouples which extended into the flowing salt near the four corners of the loop. Energy supplied to the tube furnace was increased until the maximum temperature of salt in the loop (T_{f1}) reached 598°C (1109°F). The remaining steady state thermocouple readings are documented in Table I. These readings correspond to a 1000 watt energy input to the tube furnace.

The 304 SS loop was welded from 2.54 cm (1 in) O.D. x 2.1 cm (.81 in) I. D. tubing. Flanges were welded to the top of the hot and cold legs to support the specimen trees which extended into the flow. Unsealed covers were placed over the flanges to prevent foreign material from entering the loop.

2. 316 SS Loop

The 316 SS loop is shown in Figure 5. The heat source consisted of two 30.5 cm (1 ft) clam shell heater sections surrounding the hot leg. The heaters as well as parts of the loop were covered with Fiberfrax ceramic fiber insulation material. By selectively placing the insulation along the loop and controlling the energy into the heaters it was possible to achieve the steady-state temperature distribution documented in Table I. For this temperature distribution the energy inputs into heaters 1 and 2 were 430 and 270 watts respectively.

As indicated by Figure 5, the 316 SS loop was more heavily instrumented than the 304 SS loop. In addition to measuring the salt temperature, temperature measurements were made at the tube outside wall and the annular air space between the heater and the outside wall. Thermocouples T_{f4}, T_{f5}, T_{f8}, and T_{f9} were removed prior to the insertion of the 316 SS sample trees.

The 316 SS loop was constructed using 2.54 cm (1 in) O. D. x 1.9 cm (.75 in) I. D. tubing and "tee" joints at the four corners. Specimen trees were hung from the flanges located at the top of the hot and cold legs and unsealed covers were placed over the flanges.

3. Incoloy 800 Loop

A schematic of the Incoloy 800 loop is shown in Figure 6. The loop was fabricated using 2.54 cm (1 in) O. D. x 1.9 cm (.75 in) I. D. tubing. In order to determine the effect of alternate heating strategies, an additional clam shell heater section 30.5 cm (1 ft) in length was attached to the lower horizontal leg (heater #3). However, when the final desired temperature distribution was achieved, this heater was found to be unnecessary. An adequate temperature range was obtained by insulating the loop as shown and suppling power levels of 1000 and 100 watts for heaters 1 and 2, respectively. Heater #3 was not used.

TABLE I

STEADY STATE LOOP TEMPERATURE DISTRIBUTIONS

Thermocouple Notation

T_f - Fluid temperature

T_w - Outside wall temperature

T_A - Annulus temperature between clamshell heaters and outside tube wall

I 800 Loop

Location	Temperature °C (°F)	
T_{f1}	596	(1104)
T_{f2}	559	(1038)
T_{f3}	519	(966)
T_{f4}	440	(824)
T_{f5}	355	(671)
T_{f6}	332	(630)
T_{f7}	368	(694)
T_{f8}	621	(1149)

304 SS Loop

Location	Temperature °C (°F)	
T_{f1}	598	(1109)
T_{f2}	532	(990)
T_{f3}	416	(781)
T_{f4}	330	(626)

316 SS Loop

Location	Temperature °C (°F)	
T_{f1}	602	(1115)
T_{f2}	581	(1077)
T_{f3}	550	(1022)
T_{f4}	531	(988)
T_{f5}	469	(877)
T_{f6}	371	(700)
T_{f7}	341	(645)
T_{f8}	445	(833)
T_{f9}	591	(1096)
T_{f10}	602	(1115)
T_{w1}	389	(732)
T_{w2}	451	(844)
T_{w3}	538	(1000)
T_{w4}	601	(1113)
T_{w5}	651	(1204)
T_{w6}	656	(1213)
T_{A1}	604	(1120)
T_{A2}	677	(1250)
T_{A3}	669	(1236)
T_{A4}	731	(1347)

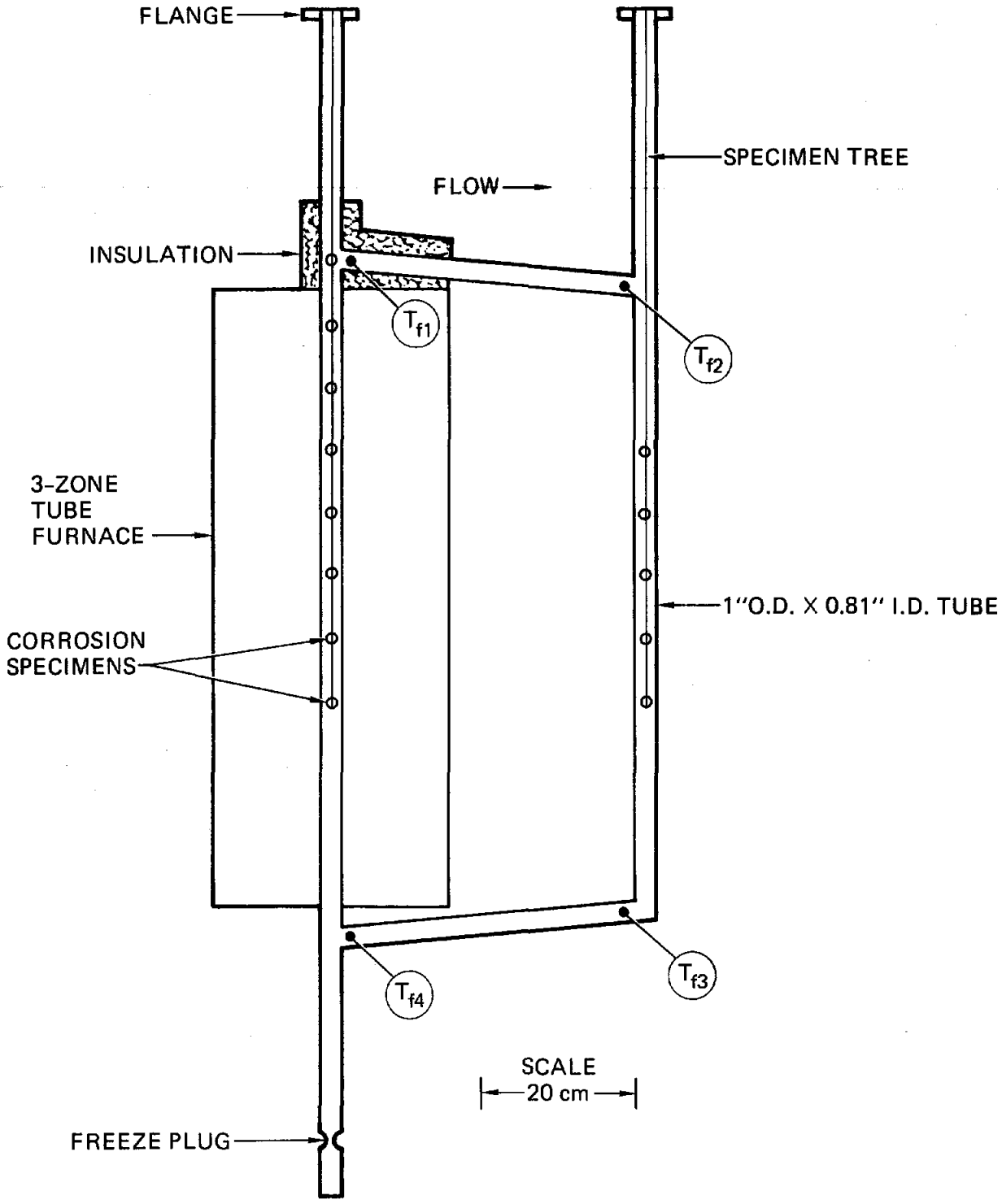

Figure 4. Schematic of 304 SS Loop

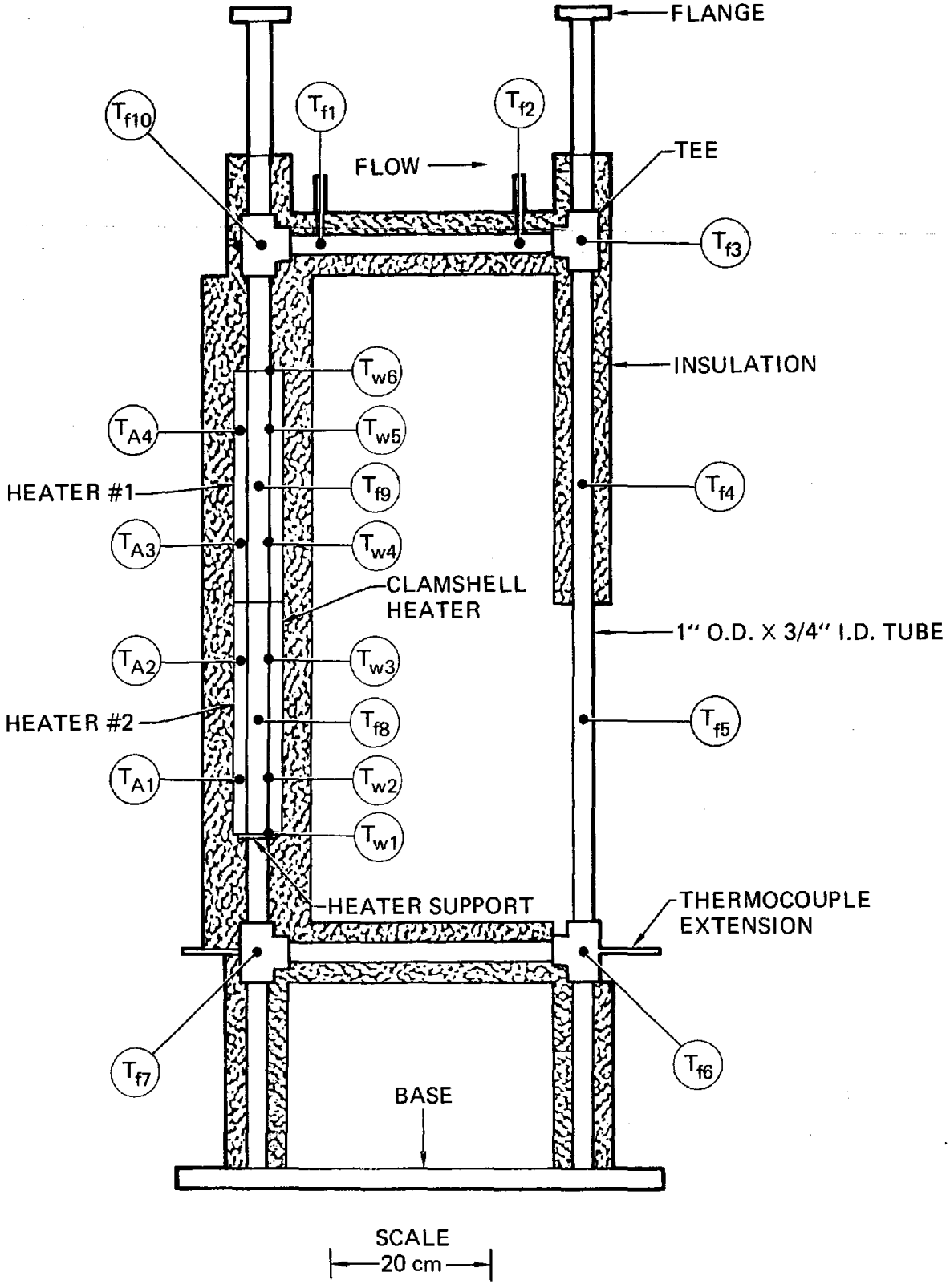

Figure 5. Schematic of 316 SS Loop

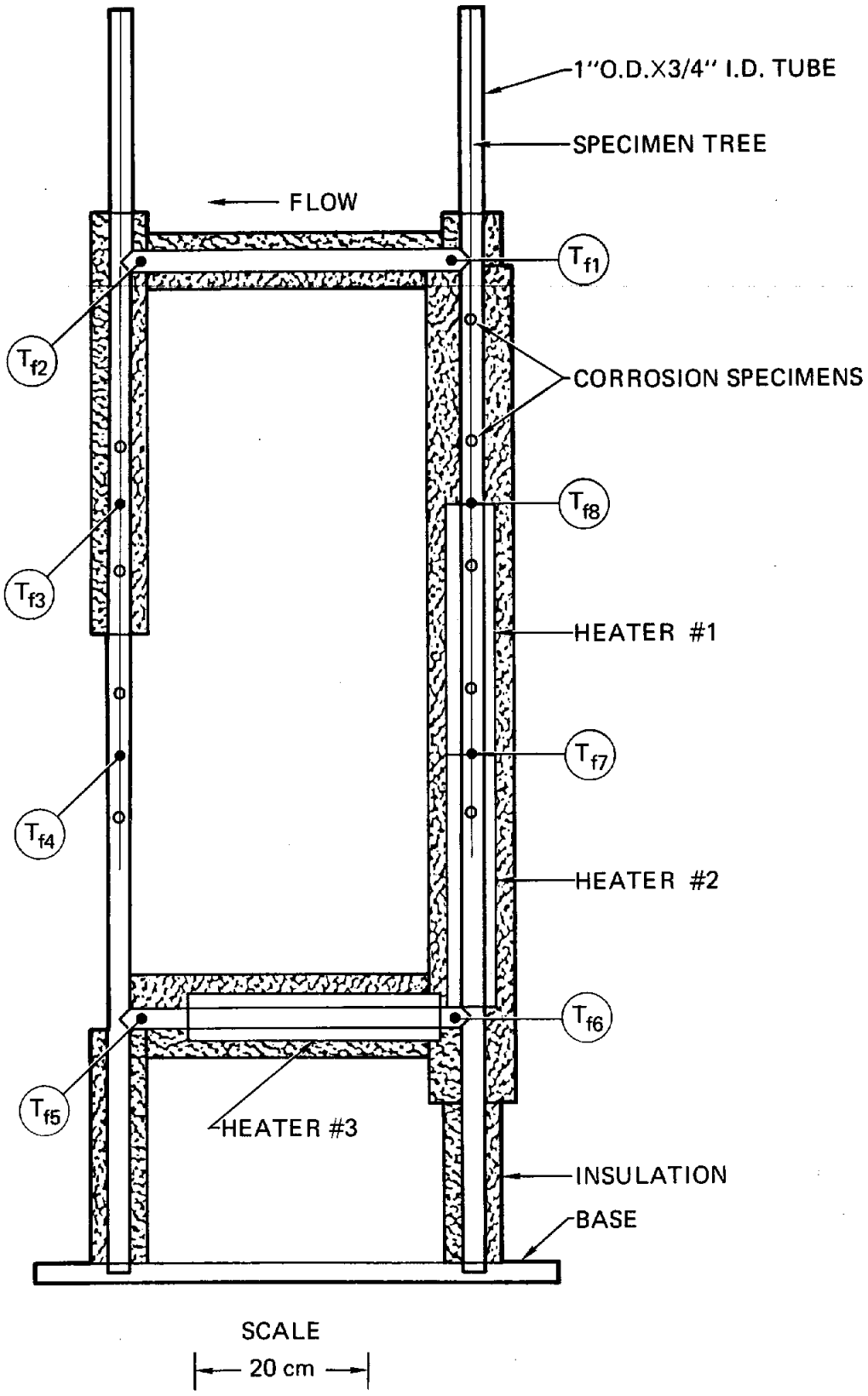

Figure 6. Schematic of Incoloy 800 Loop

The steady state temperature distribution for the loop is documented in Table I. Thermocouples T_{f3}, T_{f4}, T_{f7}, and T_{f8} were removed prior to the insertion specimen trees in the hot and cold legs. The top of each leg was covered but not sealed from the atmosphere.

C. Operating Procedures

The start-up procedure was designed to melt the salt charge while not exceeding the maximum planned steady-state temperature in the loop. The tubes were temporarily wrapped with tape trace heaters in the sections not heated by furnace elements. The trace heaters were controlled with variable transformers to limit the power input to 2 watts/in^2 (0.3 watts/cm^2). A charge of Partherm 430 (60 w/o $NaNO_3$, 40 w/o KNO_3) in the granular, as received from Park Chemical Company was weighed in an amount sufficient to fill the loop. The loop was filled with a portion of the charge and slowly melted at a temperature limit of 315°C (600°F). The remainder of the charge was added as melting proceeded.

After evolution of absorbed water vapor appeared to be complete, the power to the permanent heating elements was increased and the tape trace heaters were removed. The power inputs to the heated sections of the hot leg were then adjusted to obtain the desired values of maximum temperature and temperature difference (i.e., difference between maximum and minimum loop temperatures). The control strategy was based on the observations that: 1) the maximum loop temperature was most sensitive to the power input to the top heating section and 2) the loop temperature difference was inversely related to the power input to the lower heating elements (i.e., increasing energy to the lower heaters tended to decrease the loop temperature difference.

D. Flowrate Estimates

The low velocities and correspondingly low pressure drops characterized by convective loop flows make the direct measurement of mass flowrate and velocity difficult, if not impossible by conventional means. In the present study, salt velocities were estimated from thermocouple readings and measured heater output levels using an simple first law energy balance. In estimating flow velocities, the following assumptions were made:

1. Steady state-steady flow process through the control volume
2. Negligible changes.in kinetic and potential energy and no viscous dissipation
3. Negligible variation in temperature, velocity, or salt properties in the direction perpendicular to the flow
4. Heat loss to the surroundings over the insulated heated section assumed small compared to heat absorbed by the salt
5. Salt flowing through the control volume characterized by an "average" density, velocity, and specific heat.

Application of the first law of thermodynamics leads to the following equation for estimating salt velocity over an arbitrary control volume in the loop:

$$\bar{v} = \frac{\dot{Q}_{cv}}{A\bar{c}\bar{\rho}(T_e - T_i)}$$

where $\bar{v}$ = average velocity of salt through the control volume

A = cross-sectional flow area

$\bar{c}$ = average salt specific heat

$\bar{\rho}$ = average salt density

T_e = temperature of salt exciting the control volume

T_i = temperatures of salt entering the control volume

$\dot{Q}_{cv}$ = space averaged rate at which heat is added to the control volume

The selection of control volumes for estimating $\bar{v}$ is dictated by the positioning of thermocouples and heaters in the loop since values of T_e and T_i are obtained from thermocouple readings and the corresponding value for Q_{cv} is determined from the heater input measurements. On the 316 SS and Incoloy 800 loops the positioning of extra thermocouples in the heated section permitted two independent velocity estimates to be made. (Two independent control volumes could be selected.)

Table II contains a summary of salt velocity estimates for all three loops. The simple first law analysis gives surprisingly consistent results for the three loops. The major inconsistency in the calculations occurs for the prediction of $\bar{v}$ in the two control volume calculations for the Incoloy 800 loop. The calculation across $T_{f6} - T_{f7}$ results in a $\bar{v}$ which is

TABLE II

LOOP VELOCITY ESTIMATES FROM FIRST LAW ANALYSIS

Loop	Control Volume used in Calculation of $\bar{v}$	$\dot{Q}_{cv}$ watts (Btu/hr)	$\bar{v}$ m/hr (ft/hr)
304 SS	$T_{f4} - T_{f1}$	1000 (3410)	14.5 (47.6)
316 SS	$T_{f8} - T_{f9}$	350 (1200)	11.1 (36.4)
	$T_{f7} - Tf_{10}$	700 (2390)	12.2 (39.9)
Incoloy	$T_{f6} - T_{f7}$	100 (341)	12.3 (40.2)
800	$T_{f7} - T_{f8}$	1000 (3410)	18.1 (59.5)

32% lower than that predicted for $T_{f7} - T_{f8}$. Because of the small temperature difference measured across $T_{f6} - T_{f7}$, this calculation has the greatest uncertainty. Considering the simplicity of the calculation and the restrictiveness of the assumptions used, this method appears adequate for making "order of magnitude" estimates of velocity in the loops.

The cross-sectional flow areas for the 316 SS and Incoloy 800 loops are identical. A comparison of the predicted velocities for these two loops is consistent with the relative magnitude of heat input, i.e., the lower predicted velocity for the 316 SS loop is expected because of the lower heat input. Similarly a comparison of the $\bar{v}$ values for the 304 SS and Incoloy 800 loops (loops having nearly the same overall power input) shows a lower velocity for salt in the 304 SS loop. This too is expected since the cross-sectional flow area for that loop is greater.

In an operating solar-thermal plant, the velocity of salt being pumped through pipes and heat exchangers is expected to be on the order of 10^4 m/hr. This is, of course, three orders of magnitude greater than the velocities which can be expected in convective loop corrosion tests. Hence, while these tests supply much needed data on the corrosion effects of mass transport and a temperature gradient, no information can be obtained on erosion effects.

III. Materials Testing

A. Experimental Design and Procedure

The purpose of materials testing in thermal convection loops is to determine the corrosion rates of alloy samples located at various positions in the loop and to observe if material is transported from the hot section to the cold section. Examination of these processes requires analysis of both the inserted metallic samples and the molten salt circulating in the loop.

In the experimental design, alloy samples, consisting of rectangular coupons approximately 3/8" x 3/4" x 1/16" were suspended from removable rods which traverse the hot and cold legs. Samples were distributed uniformly along the length of the hot leg, where temperature variations were more pronounced. Additional samples were closely grouped in the relatively high temperature region at the top of the hot leg to obtain statistical data where oxidation is most rapid. Fewer specimens were used in the cold leg since the temperature range there was substantially less than the hot leg.

Several variations of the three basic alloys were studied. Weldments of each alloy were produced by the gas-tungsten-arc process. Each weldment coupon included sections of the re-solidified, heat-affected and parent zones. In addition, samples of the stabilized stainless steels, 321 SS and 347 SS, were placed in the 304 SS and 316 SS loops, respectively.

Alloy samples were prepared by grinding with 180 grit SiC paper followed by cleaning ultrasonically in a methanol-acetone mixture. After weighing and visual inspection, they were inserted into the loop. During the course of the

experiment, coupons were periodically removed, ultrasonically cleaned in distilled water, weighed, examined optically and by scanning electron microscope. Coupons were normally re-inserted after inspection, although samples were withdrawn for metallographic analysis of corrosion. Samples of the molten salt were also withdrawn periodically and chemically analyzed for metallic content (chromium, iron and nickel) as well as the nitrite/nitrate ratio and carbonate and hydroxide content.

B. Preliminary Results

Preliminary results are presented to indicate the type of information obtainable from convection loop experiments and to highlight the basic features of corrosion behavior observed to date. Subsequent reports will document the corrosion phenomena observed in detail and will evaluate the mechanisms involved to provide guidelines for projecting the lifetimes of alloys under various conditions.

The 304 SS loop has operated at a maximum temperature of 600°C (1112°F) for about 4000 hours. Relatively little corrosion has been observed and the weight changes measured for these samples were less than 0.2 mg/cm^2. In the hot leg, initially negative weight changes occur simultaneously with the appearance of adherent tarnish films on the surface of the samples, implying that the depletion of alloy elements exceeds the gain in weight due to oxidation. A slight increase in the weight of samples in the cold leg was observed.

The corrosion morphology of a 304 SS sample withdrawn from the hot leg, after 1977 hours, is shown in the photomicrograph in Figure 7. A duplex oxide layer was formed where the outer layer was Fe_3O_4. The inner oxide layer contained much more chromium, although iron remained the major metallic element. This layer is probably a spinel of the type, $(Fe,Cr)_3O_4$. The growth mechanism of the duplex oxide cannot yet be determined, but the oxide layer structure observed here is quite similar to that reported for stainless steels in CO_2 at 600°C where the oxide layers grow by outward movement of iron and chromium (24,25).

Chemical analysis of salt samples taken from the 304 loop revealed several interesting features, as shown in Table III where concentrations of chromium, NO_2^- and CO_3^{-2} are given. The analyses of salt samples withdrawn from the hot and cold legs are basically the same, an expected result since the time required for a complete fluid circulation, about 5 mintues, is much less than the time constants estimated for corrosion and decomposition reactions in the salt. The chromium content reached a value of about 80 ppm after 2045 hours and appeared to be increasing linearly with time. The iron and nickel contents were much smaller and were limited by the sensitivity of the atomic absorption spectrometer.

The concentration of NO_2^- attained a steady value of about 3 w/o after 500 hours of operation, which corresponds to the equilibrium value for the decomposition reaction, $NO_3^- = NO_2^- + 1/2\ O_2$ at the maximum temperature of the loop. The concentration of CO_3^{-2}, due to absorption of CO_2 from the atmosphere, also became steady at a value of about 0.3 w/o which is less than the minimum saturation value, corresponding to the lowest temperature in the loop (26).

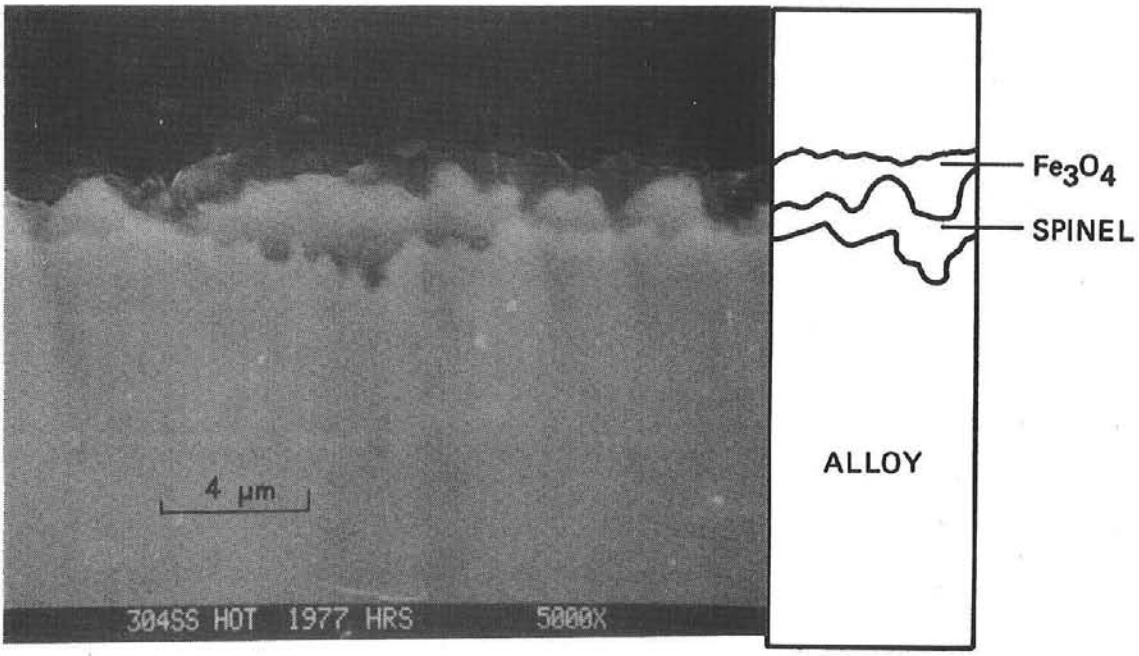

Figure 7. Microstructure of 304 SS After 1977 Hours at 600°C (1112°F)

TABLE III

CHEMICAL ANALYSIS OF SALT SAMPLES FROM 304 SS LOOP

Time (Hrs)	Leg	Cr (ppm)	NO_2^- (%)	CO_3^{-2} (%)
574	Hot	46	2.6	0.27
1102	Hot	60	3.3	0.34
	Cold	63	2.8	0.41
2045	Hot	78	3.1	0.38
	Cold	77	2.9	0.28

The 316 and 800 loops were operated at a higher maximum temperature than the 304 loop to accelerate testing and corrosion was correspondingly more rapid. Weight change plots from 316 and 800 at a maximum temperature of 640°C (1184°F) in these loops show that specimens initially gain weight but switch to a weight loss after about 2000 hours as illustrated in Figure 8. The loss of weight occurs despite the presence of adherent surface oxide layers on both alloys. This loss is attributed to rapid depletion of chromium from the alloy, which must yet be verified by chemical analysis in progress of salt samples from the loops.

A cross section of a 316 SS sample withdrawn from the hot leg after 1000 hours at 640°C (1184°F) is shown in Figure 9. The thickness of the corrosion layer increased several times compared to 304 SS at 600°C (1112°F) as shown in Figure 7. The value of the maximum temperature is somewhat uncertain, ± 15°C, since it was estimated from the temperature profile data in Table I. The corrosion products were identified as an outer layer of Fe_3O_4 and an inner layer of a chromium-containing iron oxide. Other changes, such as internal oxidation and void formation, appear to be taking place in the sub-scale region of the alloy. Future results will clarify the nature of these processes.

The corrosion products were generally adherent although spalling was found to increase on coupons exposed to higher temperatures. The formation of iron oxides and spinels implies that adherence of the surface scales will be poor under thermal cycling conditions (27). This effect may have a considerable impact on corrosion rates and should be investigated.

IV. Future Activities

Current corrosion loop testing in support of the TESSTA program is expected to continue at SLL through FY80. Corrosion and salt chemistry data will continue to be collected from all three loops until each has accumulated a minimum of 6000 hours. At that point the decision will be made to either continue testing or begin a new series of tests to study parameters such as temperature or salt additives.

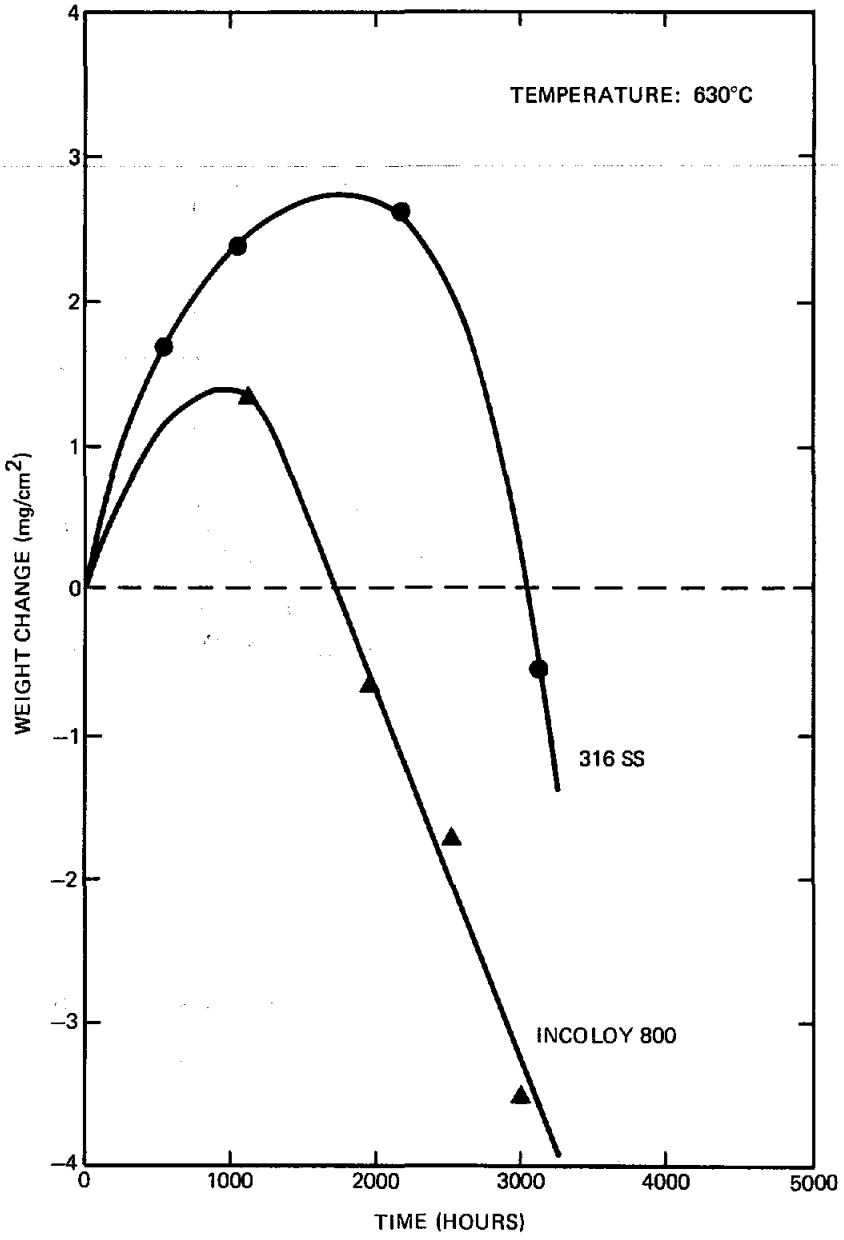

Figure 8. Weight Changes of 316 SS and IN800 at 640°C (1184°F)

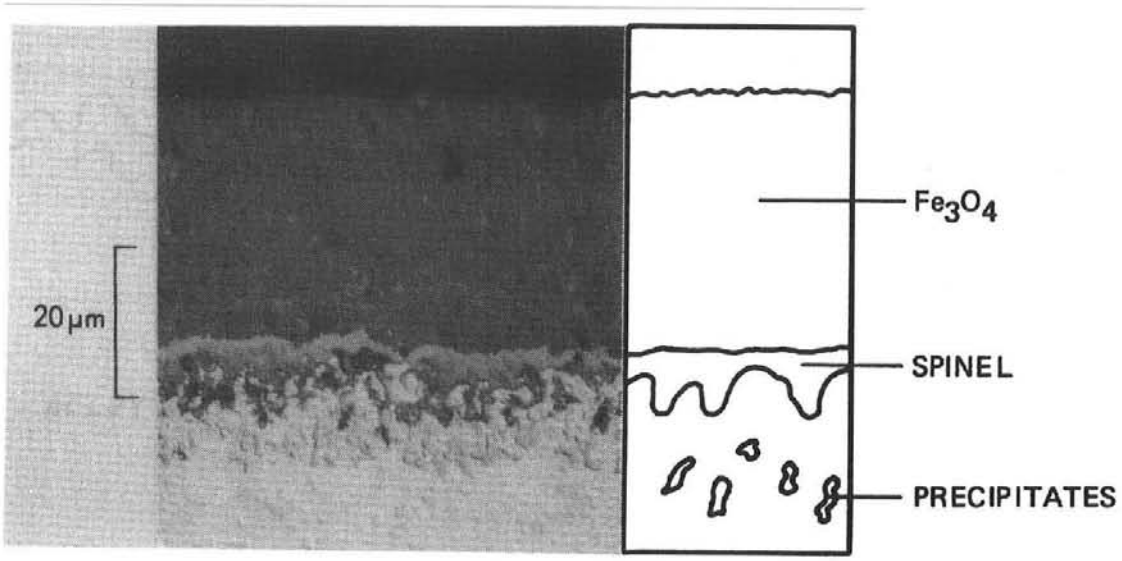

Figure 9. Corrosion Products on 316 SS After 1005 Hours at 640°C (1184°F)

To supplement the SLL in-house activities, the TESSTA program is currently funding a parallel effort at Oak Ridge National Laboratory. The ORNL program includes the construction, testing, and evaluation of three corrosion loop experiments similar to those described here. The loops will be constructed from the same three materials (304 SS, 316 SS, and Incoloy 800) and corrosion and salt chemistry data will be collected through 4500 hours of operation at a maximum temperature of 600°C. The major difference between the SLL and ORNL studies is that the ORNL loops will be sealed from the atmosphere, to simulate an alternative mode of receiver operation. Sealing the system will affect the chemical equilibrium in the molten nitrate salt significantly, and thereby may have an important influence on corrosion rates and elemental solubilities.

V. Conclusions

Convective loop experiments are a valuable and relatively simple method for assessing molten salt materials compatibility. The loops may be used to investigate the influence of mass transport and a temperature gradient on corrosion rates. Additional experiments must be performed in pumped loops, however, to evaluate erosion effects. The loops may be constructed quickly and inexpensively, and once operational, can run for thousands of hours with little operator effort.

Preliminary results concerning unsealed loops containing Partherm 430 indicate that corrosion states at temperatures less than 600°C (112°F) are quite low, although chromium is depleted from the alloys and dissolved in the molten salt. The rates of corrosion and chromium depletion increase with temperature to a degree where a loss of unaffected metal of several mils/years is estimated at 630°C - 640°C (1165°F - 1184°F). However, additional results from the experimental program in progress, as well as the sub-contracted effort at ORNL are required to fully characterize the corrosion behavior of the high temperature structural alloys considered for molten salt systems.

VI. REFERENCES

1. "A Description and Assessment of Large Solar Power Systems Technology," Complied by L. N. Tallerico, Sandia National Laboratories, Livermore, CA, SAND79-8015.

2. "Conceptual Design of Advanced Central Receiver Power System, Phase 1," Final Report for Contract EG-77-C-03-1724, Martin Marietta, Denver, CO, September 1978.

3. "Line-Focus Solar Central Power Systems," Final Report for Contract EY-76-C-03-0115, SRI International, Menlo Park, CA Report to be published.

4. "Line Focus Solar Central Power Systems, Phase I," Final Report for Contract ET-78-C-03-2240, General Atomic Company, San Diego, CA, 1979.

5. "Thermal Energy Storage Technology for Solar Thermal Power Systems - Multi-Year Program Plan," U.S. Department of Energy, Division of Energy Storage Systems and Division of Central Solar Technology. Draft for Public Comment dated March 13, 1979.

6. Brumleve, T. D., "Sensible Heat Storage in Liquids," SLL-73-0263, Sandia National Laboratories, Livermore, CA, 1974.

7. "Third Annual Proceedings of Thermal Energy Storage Contractors' Information Exchange Meetings," December 5-6, 1978, Springfield, VA, U.S. Department of Energy, Division of Energy Storage Systems, CONF-781231, 1978.

8. Hamilton, D. C., Lynch, F. E. and Palmer, L. D., "The Nature of the Flow of Ordinary Fluid in a Thermal Convection Harp," Oak Ridge National Laboratory Report, ORNL 1624, 1960.

9. Zvirin, Y. and Grief, R., "Transient Behavior of Natural Circulation Loops: Two Vertical Branches with Point Heat Source and Sink," Int. J. Heat Mass Transfer, 22, pp 499-504, 1979.

10. Japikse, D., "Advances in Thermosyphon Technology," Advances in Heat Transfer, 9, 1973.

11. Chato, J. C. and Lawrence, W. T., "Natural Convection Flows in Single and Multiple - Channel Systems," Developments in Heat Transfer, 1964.

12. Chato, J. C., "Natural Convection Flows in Parallel-Channel Systems," J of Heat Transfer, 85, November, 1963.

13. E. G. Bohlmann, "Heat Transfer Salt for High Temperature Steam Generation," ORNL-TM-3777, Oak Ridge National Laboratory, 1972, p. 16 ff.

14. C. M. Kramer, W. H. Smyrl and W. B. Estill, "Corrosion of Fe Alloys in HITEC at 823°K," SAND78-8256, Sandia National Laboratories, 1978.

15. V. P. Burolla and J. J. Bartel, "The High Temperature Compatibility of Nitrate Salts, Granite Rock and Pelletized Iron Ore," SAND79-8634, Sandia National Laboratories, 1979.

16. G. Long, "Mechanisms of Liquid-Metal Corrosion," in Corrosion, Vol. 1, L.L. Shrier, editor.

17. J. R. Keiser, J. H. DeVan and E. J. Lawrence, "Compatibility of Molten Salts with Type 316 Stainless Steel and Lithium," J. Nucl. Mater., 85, 275 (1979).

18. J. W. Koger, "Resistance to Liquid Metals, Salts and Fuel Ash Deposits," Handbook of Stainless Steels, D. Pickner and I. M. Bernstein, editors, McGraw-Hill, 1977, Ch. 18.

19. J. W. Koger, "Flouride Salt Corrosion and Mass Transfer in High Temperature Dynamic Systems," Corrosion, 29, 115 (1973).

20. J. W. Koger, "Corrosion Product Deposition in Molten Fluoride Salt Systems," Corrosion, 30, 125 (1974).

21. J. R. Keiser and J. H. DeVan, "Design and Operation of Thermal Convection Loops for Corrosion Measurements in Molten LiF-LiCl-LiBr," Corrosion/79, Paper No. 117, Atlanta, GA, National Assoc. Corrosion Eng., March 1979.

22. L. F. Grantham, and P. B. Ferry, "Corrosion in Alkali Metal Carbonate-Based Melts," Proc. International Symposium on Molten Salts, p. 270, The Electrochemical Society, 1976.

23. W. D. Manly, "Operation of a Ni-NaOH Thermal Convection Loop," ORNL CF-51-11-186, Oak Ridge National Laboratory, 1951.

24. A. F. Smith and R. Hales, "Concentration Profiles through a Duplex Oxide Grown on 316 Stainless Steel," Werkstoffe und Korrosion, 29, 246 (1970).

25. J. C. P. Garrett et al., "Some Factors in the Oxidation of Austenitic Stainless Steel," Proc. Intl. Conference on Corrosion of Steels in CO_2," British Nuclear Energy Society., 1974, p. 298.

26. P. G. Zambonin, "On the Voltammetric Behavior of the Carbon Dioxide-Oxygen-Carbonate System in Molten Alkali Nitrates," Analyt. Chem., 44, 763 (1972).

27. A. J. Sedricks, Corrosion of Stainless Steels, Wiley, 1979, p. 237 ff.

APPENDIX A--MATERIALS LIST AND COST ESTIMATE FOR A TYPICAL CONVECTIVE LOOP

	LOOP	PRICE	QUANTITY	COST
1.	1" O.D. x 3/4" I.D. Tube	$18.00/ft	13 ft.	$234
	Machining			190
2.	Stand	10.00/ft	2 ft.	20
	Machining			40
3.	Salt	.30/lb	10 lb.	3
	HEATING			
4.	Heaters	13.30/ea	8 ea.	106
5.	Voltage Controllers	66.50/ea	2 ea.	133
6.	Wire and Plugs			15
7.	Insulation	2.00/ft^2	13 ft^2	26
	TEMPERATURE MEASUREMENT			
8.	Digital Thermometer	340.00/ea	1 ea.	340
9.	Thermocouples	16.92/ea	4 ea.	67
10.	Thermocouple Fittings	6.10/ea	4 ea.	24
11.	1/4" Tube	5.00/ft	1 ft.	5
	STARTUP			
12.	Tape Heaters	24.58/ea	4 ea.	98
	SAMPLING			
13.	Sample Tree			50
	LABOR			
14.	Weld Shop	30.00/hr	2 hr.	60
15.	Assembly	10.00/hr	40 hr.	400
			TOTAL	$1813

UNLIMITED RELEASE

INITIAL DISTRIBUTION:

TIC/UC62 (316)

USDOE (5)
Division of Energy Storage Systems
Washington, D. C. 20545
Attn: G. Pezdirtz
J. H. Swisher
J. Gahimer
R. Scheithauer
W. Frier

USDOE
Albuquerque Operations Office
Special Programs Division
P. O. Box 5400
Albuquerque, NM 87115
Attn: D. Krinz

NASA-Lewis Research Center (2)
Cleveland, OH 44101
Attn: A. W. Nice
J. Calogeras

Oak Ridge National Laboratory
Oak Ridge, TN 37830
Attn: J. DeVan

USDOE (3)
San Francisco Operations Office
1333 Broadway
Oakland, CA 94612
Attn: J. Blasy
R. Hughey
D. Elliott

USDOE (4)
Division of Solar Technology
Washington D. C. 20545
Attn: G. W. Braun
M. U. Gutstein
G. M. Kaplan
J. E. Rannels
J. Dollard
W. Auer

Aerospace Corporation (2)
2350 El Segundo Blvd.
El Segundo, CA 90009
Attn: E. Katz
P. Mathur

JPL (4)
4800 Oak Grove Dr.
Pasadena, CA 91103
Attn: V. Truscello
R. Manvi
D. Young
J. Becker

EPRI (2)
P. O. Box 10412
3412 Hillview Ave.
Palo Alto, CA 94303
Attn: J. Bigger
T. R. Schneider

SERI (3)
1536 Cole Blvd.
Golden, CO 80401
Attn: K. Touryan
B. Gupta
C. Wyman

C. Winter, 400
A. Narath, 4000
J. H. Scott, 4700
G. E. Brandvold, 4710; Attn: B. W. Marshall, 4713
R. P. Stromberg, 4714
V. L. Dugan, 4720; Attn: J. V. Otts, 4721
J. F. Banas, 4722
J. A. Leonard, 4725
J. K. Galt, 5000
R. S. Claassen, 5800
R. G. Kepler, 5810
M. J. Davis, 5830
N. J. Magnani, 5840; Attn: D. W. Schaefer, 5841

T. B. Cook, 8000
W. J. Spencer, 8100
W. E. Alzheimer, 8120
R. J. Gallagher, 8124
W. S. Winters, Jr., 8124 (6)
A. N. Blackwell, 8200
B. F. Murphey, 8300
D. M. Schuster, 8310;
W. R. Hoover, 8312
R. W. Mar, 8313
R. W. Bradshaw, 8313 (6)
A. S. Nagelberg, 8313
A. J. West, 8314
L. A. West, 8315
J. C. Swearengen, 8316
R. Rinne, 8320
L. Gutierrez, 8400

C. S. Selvage, 8420
R. C. Wayne, 8450
J. Genoni, 8450
P. J. Eicker, 8451
A. C. Skinrood, 8452
W. G. Wilson, 8453
R. W. Carling, 8453
L. G. Radosevich, 8453 (2)
F. W. Hart, 8453 (6)
Publications Division, 8265, for TIC (2)
Publications Division, 8265/Technical Library Processes Division, 3141
Technical Library Processes Division, 3141 (2)
Library and Security Classification Divsion, 8266 (3)